Chapter 5

3D Numerical Study of Metastatic Tumor Blood Perfusion and Interstitial Fluid Flow Based on Microvasculature Response to Inhibitory Effect of Angiostatin

Gaiping Zhao

Additional information is available at the end of the chapter

http://dx.doi.org/10.5772/intechopen.78949

Abstract

Metastatic tumor blood perfusion and interstitial fluid transport based on 3D microvasculature response to inhibitory effect of angiostatin are investigated. 3D blood flow, interstitial fluid transport, and transvascular flow are described by the extended Poiseuille's, Darcy's, and Starling's law, respectively. The simulation results demonstrate that angiostatin has the capacity to regulate and inhibit the formation of new blood vessels and has an obvious impact on the morphology, growth rate, and the branches of microvascular network inside and outside the metastatic tumor. Heterogeneous blood perfusion, widespread interstitial hypertension, and low convection within the metastatic tumor have obviously improved under the inhibitory effect of angiostatin, which suits well with the experimental observations. They can also result in more efficient drug delivery and penetration into the metastatic tumor. The simulation results may provide beneficial information and theoretical models for clinical research of antiangiogenic therapy strategies.

Keywords: blood perfusion, interstitial transport, metastatic tumor, angiostatin, 3D simulation

1. Introduction

Cancer is the second leading cause of mortality worldwide [1], right behind cardiovascular disease. Metastatic tumors, the ultimate causes of death for the majority of cancer patients, are the important biological characteristics of malignant tumors. Metastasis occurs when cancer

cells spread from a primary tumor to distant and vital organs (secondary sites) in human body. Angiogenesis is necessary for tumor growth, invasion, and metastasis [2], since it supplies the nutrients and oxygen for continued tumor growth. The neovascularization accelerates the growth of tumor while simultaneously offering an initial route by which cancer cells can escape from a primary tumor to form metastatic tumor. Cancer cells migrate into the blood stream and surrounding tissues via microcirculation, then continue to grow giving rise to metastases [3]. The blood perfusion and interstitial fluid flow have been recognized as critical elements in metastatic tumor growth and vascularization [4]. However, tumor vessels are dilated, saccular, tortuous, and heterogeneous in their spatial distribution. These abnormalities result in heterogeneity of blood flow and elevated interstitial fluid pressure (IFP), which forms a physiological barrier to the delivery of therapeutic agents to tumors [5]. Abnormal microvasculature and microenvironment further lowers the effectiveness of therapeutic agents.

Experimental research showed that the primary tumor in the Lewis lung model system was capable of generating a factor which was named angiostatin later suppressing the neovascularization and expansion of tumor metastases [6]. Angiostatin is a 38-kD internal peptide of plasminogen, which is a potent inhibitor of angiogenesis in vivo, and selectively inhibits endothelial cell (EC) proliferation and migration in vitro. Tumor cells express enzymatic activity which is capable of hydrolyzing plasminogen to generate angiostatin [7]. Angiostatin is then transported and accumulated in the blood circulation in excess of the stimulators and thus inhibiting angiogenesis of a metastatic tumor. Angiostatin, by virtue of its longer half-life in the circulation [8], reaches the vascular bed of metastatic tumor. As a result, growth of a metastasis is restricted by preventing and inhibiting angiogenesis within the vascular bed of the metastasis itself. A schematic diagram of this process is given in **Figure 1**. Indeed, antiangiogenic treatments directly targeting angiogenic signaling pathways as well as indirectly modulating angiogenesis show normalization of tumor microvasculature and microenvironment at least transiently in both preclinical and clinical settings.

In spite of several mathematical models of metastatic tumors, there appears to be little in the literature by way of mathematical modeling of the mechanisms of antiangiogenic activity of angiostatin on blood flow and interstitial fluid pressure in a metastatic tumor. Liotta et al. [9] first

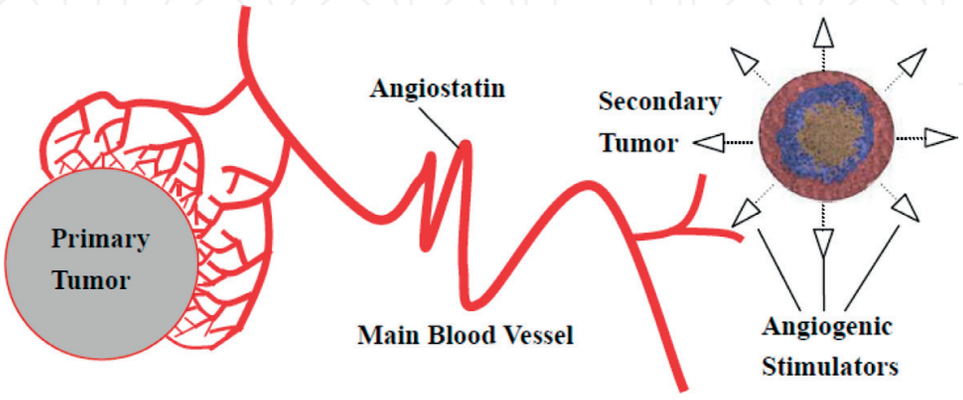

Figure 1. Schematic representation of angiostatin transported from a fully vascularized primary tumor to its relation to a distant secondary tumor.

http://dx.doi.org/10.5772/intechopen.78949

developed an experimental model to quantify some of the major processes initiated by tumor transplantation and culminating in pulmonary metastases. The study suggested that "dynamics of hematogenously initiated metastases depended strongly on the entry rate of tumor cell clumps into the circulation, which in turn was intimately linked to tumor vascularization." Later in the study, Liotta et al. [9] confirmed their former observation and raised the idea that "larger clumps produce significantly more metastatic foci than do smaller clumps matched for the number of cells." Saidel et al. [10] proposed a lumped-parameter, deterministic model of the hematogenous metastatic process from a solid tumor, which provided a general theoretical framework for analysis and simulation. Numerical solutions of the model were in good agreement with their experimental results [9]. The possibilities of anti-invasion and antimetastatic strategies in cancer treatment have bestowed an added preponderance with the keen interest in the mathematical modeling in the areas of tumor invasion and metastasis. Orme and Chaplain [11] presented a simple mathematical model of the vascularization and subsequent growth of a solid spherical tumor and gave a possible explanation for tumor metastasis, whereby tumor cells entered the blood system and secondary tumor may rise with the transportation function of blood. Sleeman and Nimmo [12] modified the model of fluid transport in vascularized tumors by Baxter and Jain [13] to take tumor invasion and metastasis into consideration. Although these models did provide some features of tumor metastasis and interstitial fluid transportation such as perturbation analysis, they lacked in providing more detail information of metastatic tumor and as such were of limited predicted value. More realistic models of metastasis and interstitial fluid transportation were developed to better understand its mechanism. Anderson et al. [14] presented a discrete model from the partial differential equations of the continuum models which implied that haptotaxis was important for tumor metastasis. Iwata et al. [15] proposed a partial differential equation (PDE) that described the metastatic evolution of an untreated tumor, and its predicted results agreed well with successive data of a clinically observed metastatic tumor. Benzekry et al. [16] proposed an organism-scale model for the development of a population of secondary tumors that takes into account systemic inhibiting interactions among tumors due to the release of a circulating angiogenesis inhibitor. Baratchart et al. [17] derived a mathematical model of spatial tumor growth compared with experimental data and suggested that the dynamics of metastasis relied on spatial interactions between metastatic lesions. Stéphanou et al. [18] investigated chemotherapy treatment efficiency by performing a Newtonian fluid flow simulation based on a study of vascular networks generated from a mathematical model of tumor angiogenesis. Wu et al. [19] extended the mathematical model into a 3D case to investigate tumor blood perfusion and interstitial fluid movements originating from tumor-induced angiogenesis. Soltani and Chen [20] first studied the fluid flow in a tumor-induced capillary network and the interstitial fluid flow in normal and tumor tissues. The model provided a more realistic prediction of interstitial fluid flow pattern in solid tumor than the previous models. Some related works have been done on tumor-induced angiogenesis, blood perfusion, and interstitial fluid flow in the tumor microenvironment by using 2D mathematical methods [5, 21–23]. In spite of the valuable body of work performed in simulation of blood perfusion, interstitial fluid flow, and metastasis, previous studies have not examined blood perfusion and interstitial fluid pressure in the metastatic tumor microcirculation based on the 3D microvascular network response to the inhibitory effect of angiostatin which plays a significant role in suppressing tumor growth and metastasis.

Metastatic tumor blood perfusion and interstitial fluid transport based on 3D microvasculature response to inhibitory effect of angiostatin are investigated for exploring the suppression of metastatic tumor growth by the primary tumor. The abnormal geometric and morphological features of 3D microvasculature network inside and outside the metastatic tumor, and relative complex and heterogeneous hemodynamic characteristics in the presence and absence of angiostatin can be studied in the 3D case. The simulation results may provide beneficial information and theoretical basis for clinical research on antiangiogenic therapy.

2. 3D mathematical models

2.1. Metastatic tumor angiogenesis

3D mathematical model we present in this section originates from the previous 2D tumor antiangiogenesis mathematical model [5, 21] describing how capillary networks form in a metastatic tumor in response to angiostatin released by a primary tumor. The conservation equation of endothelial cells (EC) indicates the migration of EC influenced mainly by four factors: random motility, inhibitory effect of angiostatin, chemotaxis, and haptotaxis. Subsequently, from a discretized form of the partial differential equations governing endothelial-cell motion, a discrete biased random-walk model will be derived enabling the paths of individual endothelial cells located at the sprout tips, and hence the individual capillary sprouts, to be followed. Hence, realistic capillary network structures were generated by incorporating rules for sprout branching and anastomosis. The generated microvascular network inside and outside the metastatic tumor in the presence of angiostatin and in the absence of angiostatin is shown in **Figure 2**. General morphological features of the network such as growth speed, capillary number, vessel branching order, and anastomosis density in/outside the metastatic tumor are consistent with the physiologically observed results, which indicate that angiostatin secreted by the primary tumor dose has an inhibitory effect on metastatic tumor [5, 11].

2.2. Blood perfusion

To calculate blood flow through a given 3D microvascular network of interconnected capillary elements to the metastatic tumor, assuming flux conservation and incompressible flow at each junction where the capillary elements meet

$$\sum_{n=1}^{6} Q^{n}_{(l.m.j)} \cdot B^{n}_{(l.m,j)} = 0 \tag{1}$$

where $B^{n}_{(l,m,j)}$ takes the integer 1 or 0, representing the connectivity between node (l, m, j) and its adjacent node n. $Q^{n}_{(l,m,j)}$ is the flow rate from node (l, m, j) to node n and is given by $Q^{n}_{(l.m,j)} = Q^{n}_{v,(l,m,j)} - Q^{n}_{t,(l,m,j)}$, where $Q^{n}_{v,(l,m,j)}$ is the vascular flow rate without fluid leakage, described locally by Poiseuille's law

$$Q^{n}_{v,(l.m,j)} = \frac{\pi R_n^4 \left(p_{v,(l,m,j)} - p_{v,(n)}\right)}{8\,\mu_n\,\Delta L_n} \tag{2}$$

and $Q^{n}_{t,(l,m,j)}$ is the transvascular flow rate, following Starling's law

http://dx.doi.org/10.5772/intechopen.78949

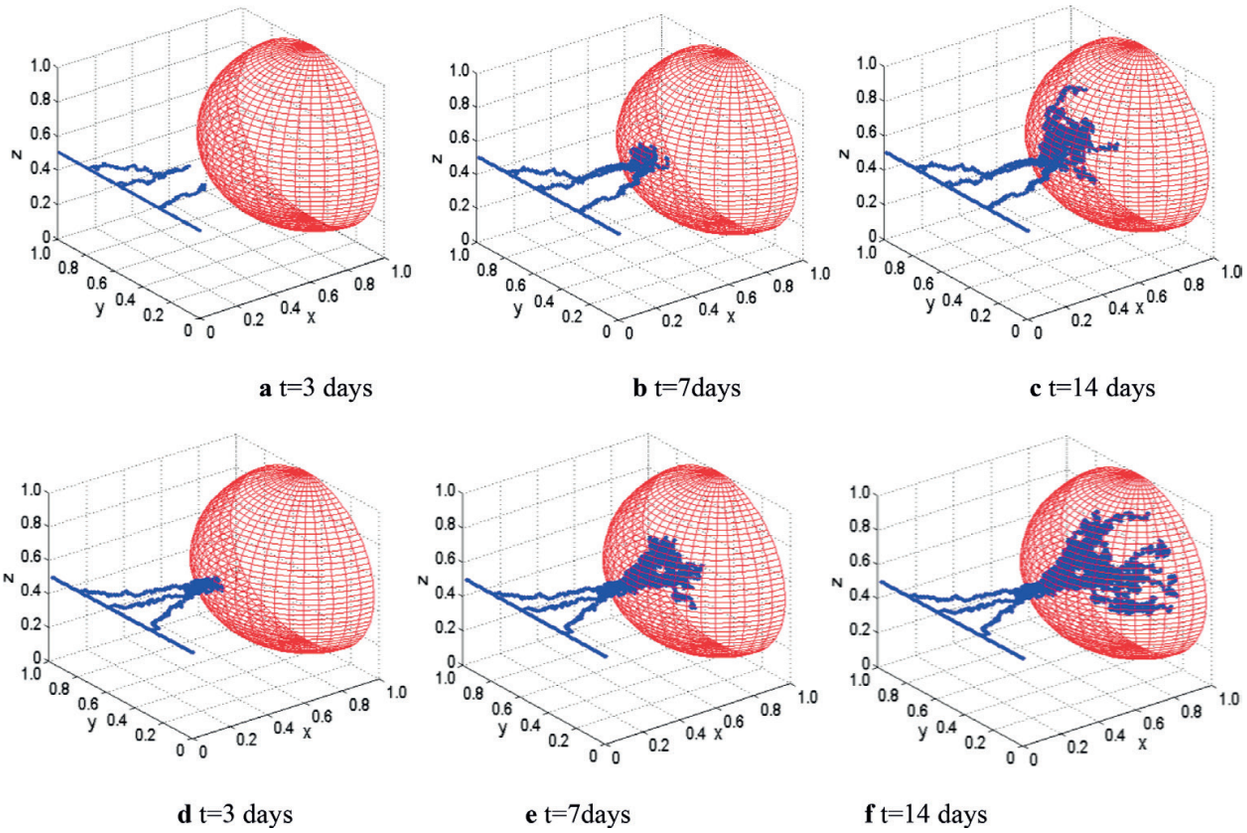

Figure 2. The spatiotemporal dynamic growth of 3D microvascular networks inside and outside the metastatic tumor: (a–c) in the presence of angiostatin; (d–f) in the absence of angiostatin.

$$Q^{n}_{t,(l,m,j)} = 2\pi R_n \Delta L_n \cdot L_{pv}\left[\left(\bar{p}^{\,n}_{v,(l,m,j)} - \bar{p}^{\,n}_{i,(l,m,j)}\right) - \sigma_t(\pi_v - \pi_i)\right] \tag{3}$$

where $p_{v,(l,m,j)}$ and $p_{v,(n)}$ are the intravascular pressure of node (l, m, j) and node n; $\bar{p}^{\,n}_{v,(l,m,j)}$ is the mean pressure in vascular element (l, m, j); $\bar{p}^{\,n}_{i,(l,m,j)}$ is the mean interstitial pressure outside of vascular element (l, m, j). μ_n, R_n, and ΔL_n are the blood viscosity, radius, and length of the vessel element n, respectively; L_{pv} is the hydraulic permeability of vascular wall; σ_t is the average osmotic reflection coefficient for plasma proteins; π_v and π_i are the colloid osmotic pressure of plasma and interstitial fluid.

2.3. Interstitial flow in metastatic tumor

Considering the metastatic tumor tissue as an isotropic porous medium, its interstitial flow is modeled by Darcy's law [24]:

$$\boldsymbol{u}_i = -\kappa \nabla p_i \tag{4}$$

where $\boldsymbol{u}_i$ is the interstitial fluid velocity; κ is the hydraulic conductivity coefficient of the interstitium; p_i is the interstitial pressure.

The continuity equation is given by:

$$\nabla \cdot \boldsymbol{u}_i = \phi_v - \phi_L \tag{5}$$

where $\phi_v = \frac{L_{pv} S_v}{V}(p_v - p_i - \sigma_t(\pi_v - \pi_i))$ is the fluid source term leaking from blood vessels. $\phi_L = \frac{L_{pL} S_L}{V}(p_i - p_L)$ is the lymphatic drainage term, which is proportional to the pressure difference between the interstitium and the lymphatics.

Mass conservation at each junction where the interstitial fluid pressure satisfies equation:

$$\nabla^2 p_i = \frac{\alpha^2}{R^2}(p_i - p_{ev}) \cdot B \tag{6}$$

where $p_{ev} = \left(L_{pv} S_v(p_v - \sigma_t(\pi_v - \pi_i)) + L_{pL} S_L p_L\right)/\left(L_{pv} S_v + L_{pL} S_L\right)$ is the effective pressure and $\alpha = R\sqrt{\left(L_{pv} S_v + L_{pL} S_L\right)/\kappa V}$ is the ratio of interstitial to vascular resistances to fluid flow. L_{pL} is the hydraulic permeability of lymphatic vessel wall. S_v/V and S_L/V are the surface areas of blood vessel wall and lymphatic vessel wall per unit volume of tissue. In the model, $L_{pL} S_L/V$ is assumed zero for tumor tissue, and given a uniform value for normal tissue referring to Baxter and Jain [13]. The continuity of pressure and flux on the interconnected boundary between the tumor and normal tissue Γ: $p_i|_{\Gamma^-} = p_i|_{\Gamma^+}$, $-\kappa_T \nabla p_i|_{\Gamma^-} = -\kappa_N \nabla p_i|_{\Gamma^+}$, κ_T, and κ_N are the hydraulic conductivity coefficients of normal tissue and tumor tissue, respectively.

Table 1 shows the values of the parameters used in the microcirculation simulations.

Parameter	Name	Value	Parameter	Name	Value
σ_t[a]	Average osmotic reflection coefficient for plasma proteins	$8.7 \times 10^{-5}{}_T$ 091_N	κ[a]	Hydraulic conductivity coefficient of interstitium	$2.5 \times 10^{-7}{}_T$ cm²/mmHg s $2.5 \times 10^{-7}{}_N$ cm²/mmHg s
π_v[a]	Colloid osmotic pressure of plasma	198_T mmHg 20_N mmHg	$\left(\frac{S_v}{V}\right)$[a]	Surface area per unit volume for transport in interstitium	50_T cm^{-1} 50_N cm^{-1}
p_L[c]	Lymphatic pressure	0.5_N mmHg	$\frac{L_{pL} S_L}{V}$[c]	Absorption capacity of lymphatic system	0_T 1/mmHg s $1.0 \times 10^{-4}{}_N$ 1/mmHg s
π_i[a]	Colloid osmotic pressure of interstitium	173_T mmHg 10_N mmHg	L_{pv}[a]	Hydraulic permeability of vascular wall	$1.86 \times 10^{-6}{}_T$ cm/mmHg s $3.6 \times 10^{-8}{}_N$ cm/mmHg s
μ[b]	Blood viscosity	1.0 cP			

[a]Jain et al. [5].

[b]Stephanou et al. [18].

[c]Zhao et al. [25].

Subscript "N" and "T" represents the values in normal and tumor tissues, respectively.

Table 1. Baseline parameter values used in the simulations.

3. Simulation results

3.1. 3D blood perfusion of metastatic tumor

We simulated the evolution of blood flow pressure in the presence/absence of angiostatin for 14 days representing the typical timescale for tumor vasculature to grow. **Figure 3** shows

http://dx.doi.org/10.5772/intechopen.78949

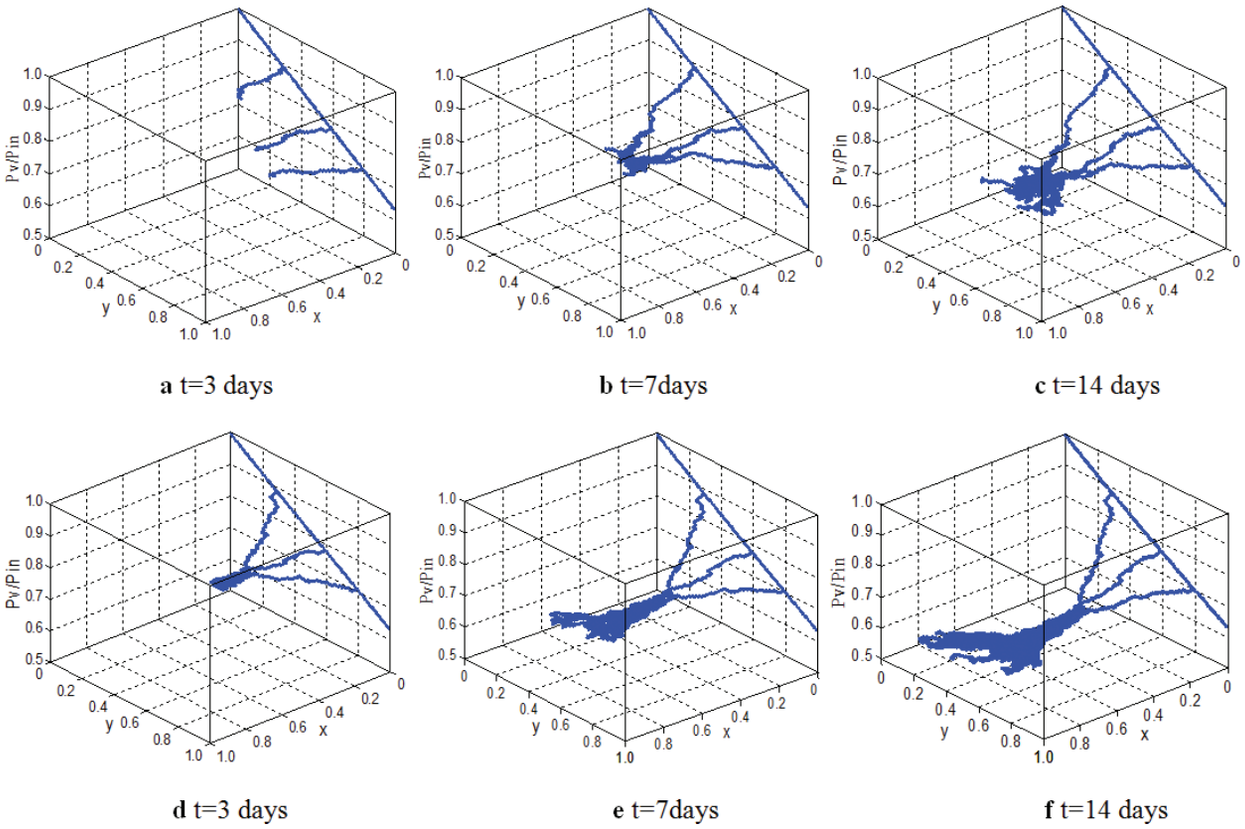

Figure 3. Simulations of blood pressure through 3D microvascular networks over time: (a–c) example simulation with angiostatin; (d–f) example simulation without angiostatin. Simulation domain is [0, 1] × [0, 1] × [0, 1]. Blood enters the networks at the end of the parent vessel ($x = 0, y = 0, z = 0.5$), distributes throughout the capillary network, leaves from the end of the parent vessel ($x = 0, y = 1, z = 0.5$).

the snapshots of the pressure profiles of blood flow through each vessel segment in a three-dimensional microvascular networks. We keep the inlet pressure and outlet pressure across parent vessel fixed at 25 and 16 mmHg [25] in the simulation, in accordance with physiological values at the capillary scale. **Figure 3** highlights a direct comparison of blood pressure distributions (**Figure 3a–c** shows the blood pressure distribution in the presence of angiostatin, **Figure 3d–f** shows the blood pressure distribution in the absence of angiostatin). We observe that the overall blood pressure is higher in the presence of angiostatin than that in the absence of angiostatin over the same growth duration. The blood flow distribution is complex and chaotic which makes the variety of blood pressure small in the interior of the metastatic tumor compared to its exterior, contributing to the difficulties of efficient drug delivery in metastatic tumor. In the presence of angiostatin, the pressure-flows within some of the daughter vessels are elevated from the branching points to the metastatic tumor surface which provides effective blood perfusion and thus efficient therapeutic agents to the tumor. The simulation results indicate that blood perfusion varies significantly with the complex and chaotic three-dimensional microvascular networks inside and outside the metastatic tumor. The poor blood perfusion can be improved through the increased intravascular pressure with the presence of angiostatin. These results suggest that the inhibitory effect of angiostatin can affect the distribution of blood flow pressure and improve drug delivery to tumor.

3.2. 3D interstitial fluid flow of metastatic tumor

Figure 4 shows the distribution of interstitial fluid pressure (IFP) within the metastatic tumor under the two mentioned situations. From the simulation results, we obtain that maximum IFP near the tumor center significantly dropped from 3.3, 11.48, and 11.53 to 0, 4.7, and 10.3 mmHg

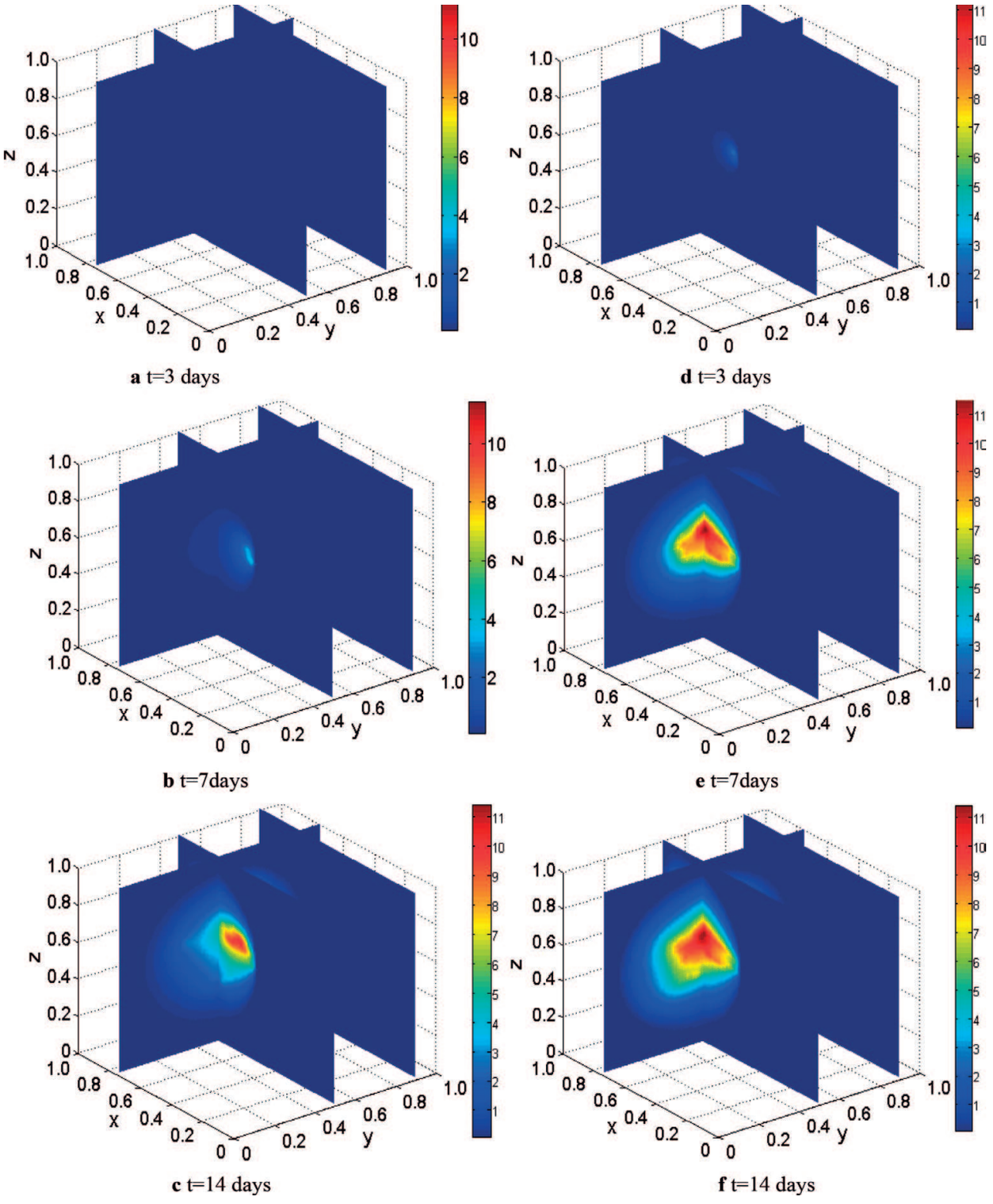

Figure 4. Interstitial fluid pressure distributions within the metastatic tumor: (a–c) in the presence of angiostatin; (d–f) in the absence of angiostatin on the same other conditions.

with the presence of angiostatin at t = 3, 7 and 14 days, respectively, which indicated the IFP plateau is well relieved. As the growth days increase, IFP gradually elevates throughout the 3D metastatic tumor and the high pressure zone is at the center of the tumor and diminishes to the periphery and later becomes flatter. Comparing **Figure 4a–c** to **Figure 4d–f**, we come to conclude that angiostatin decreases the high IFP in the tumor, thus with the lower transvascular pressure in the 3D heterogeneous capillary networks, leading to an significantly improved situation for interstitial convection which plays a significant role in nonuniform distribution of drug delivery to the metastatic tumor. These results provide important references for cancer prevention and treatment. Furthermore, antiangiogenic therapies can normalize tumor vasculature and microenvironment, at least transiently in both preclinical and clinical settings [5].

4. Conclusion

The inhibitory effect of angiostatin on the growth of metastatic tumor has been observed in some clinical and experimental malignancies. In this chapter, we develop three-dimensional mathematical models describing the metastatic tumor microvasculature and microenvironment to investigate the inhibitory effect of antiangiogenic factor angiostatin secreted by the primary tumor on metastatic tumor angiogenesis, blood perfusion, and interstitial fluid flow. Simulation results demonstrate that angiostatin has an obvious impact on the morphology, expansion speed, capillary number, and vessel branching order inside and outside the metastatic tumor. 2D and 3D mathematical models of tumor antiangiogenesis predict similar morphological behavior, such as vessels' length, branching patterns, anastomosis density, or geometric distribution, for metastatic tumor angiogenesis under the inhibitory efficiency of angiostatin. However, capillary number and microvascular density due to space growth of vessel networks are increased in the 3D model. Furthermore, the simulations reflect the influences of heterogeneous blood perfusion, widespread interstitial hypertension, and low convection within the 3D metastatic tumor by carrying out a comparative study relating to the inhibitory effect of angiostatin. We find that 2D antiangiogenesis model may be well suited to studying morphological behavior of vessel networks in the metastatic tumor, but 3D antiangiogenesis model can better analyze blood perfusion, interstitial fluid flow, or oxygen and nutrient transport within the metastatic tumor microenvironment based on its more realistic 3D microvascular networks. Although 3D simulation results are consistent with the experimental observed facts and can provide more detailed space information, however, angiogenesis and hemodynamics in the metastatic tumor by the antiangiogenic therapy are very complex. To further research tumor angiogenic mechanisms and help to improve antiangiogenic cancer therapy, more realistic features and complex biology factors need to be incorporated within the 3D model, such as the anatomy and physiology of the metastatic tumor, drug delivery of antiangiogenic therapy, behaviors of cells adhesion and interaction and coupled with the various factors or other therapy strategies.

Acknowledgements

This research is supported by the National Natural Science Foundation of China (No. 11502146), Shanghai Natural Science Foundation (No. 15ZR1429600).

Conflict of interest

The authors declare that there is no conflict of interest regarding the publication of this chapter.

Author details

Gaiping Zhao

Address all correspondence to: zgp_06@126.com

School of Medical Instrument and Food Engineering, University of Shanghai for Science and Technology, Shanghai, China

References

[1] Siegel R, Naishadham D, Jemal A. Cancer statistics 2013. CA: A Cancer Journal for Clinicians. 2013;**63**:11e30

[2] Folkman J. Tumor angiogenesis: Therapeutic implications. New England Journal of Medicine. 1971;**285**(10):1182-1186

[3] Konjevi G, Stankovi S. Matrix metalloproteinases in the process of invasion and metastasis of breast cancer. Archive of Oncology. 2006;**14**(3-4):136-140

[4] Heldin CH, Rubin K, Pietras K, Ostman A. High interstitial fluid pressure—An obstacle in cancer therapy. Nature Reviews Cancer. 2004;**4**(10):806-813

[5] Jain RK, Tong RT, Munn LL. Effect of vascular normalization by antiangiogenic therapy on interstitial hypertension, peritumor edema, and lymphatic metastasis: Insights from a mathematical model. Cancer Research. 2007;**67**(6):2729-2735

[6] O'Reilly MS, Holmgren L, Shing Y, Chen C, Rosenthal RA, Moses M, Lane WS, Cao YH, Sage EH, Folkman J. Angiostatin: A novel angiogenesis inhibitor that mediates the suppression of metastases by a Lewis lung carcinoma. Cell. 1994;**79**:315-328

[7] Sim BKL, O'Reilly MS, Liang H, Fortier AH, He W, Madsen JW, Lapcevich R, Nancy CA. A recombinant human angiostatin protein inhibits experimental primary and metastatic cancer. Cancer Research. 1997;**57**(7):1329-1334

[8] Paweletz N, Knierim M. Tumor-related angiogenesis. Critical Reviews in Oncology/Hematology. 1989;**9**(3):197-242

[9] Liotta LA, Kleinerman J, Saidel GM. Quantitative relationships of intravascular tumor cells, tumor vessels, and pulmonary metastases following tumor implantation. Cancer Research. 1974;**34**(5):997-1004

[10] Saidel GM, Liotta LA, Kleinerman J. System dynamics of a metastatic process from an implanted tumor. Journal of Theoretical Biology. 1976;**56**(2):417-434

[11] Orme ME, Chaplain MAJ. A mathematical model of vascular tumour growth and invasion. Mathematical and Computer Modelling. 1996;**23**(10):43-60

[12] Sleeman BD, Nimmo HR. Fluid transport in vascularized tumours and metastasis. IMA Journal of Mathematics Applied in Medicine and Biology. 1998;**15**(1):53

[13] Baxter LT, Jain RK. Transport of fluid and macromolecules in tumors. I. Role of interstitial pressure and convection. Microvascular Research. 1989;**37**(1):77-104

[14] Anderson ARA, Chaplain MAJ, Newman EL, Steele RJC, Thompson AM. Mathematical modeling of tumour invasion and metastasis. Journal of Theoretical Medicine. 2000;**2**(2): 129-154

[15] Iwata K, Kawasaki K, Shigesada N. A dynamical model for the growth and size distribution of multiple metastatic tumors. Journal of Theoretical Biology. 2000;**203**(2):177-186

[16] Benzekry S, Gandolfi A, Hahnfeldt P. Global dormancy of metastases due to systemic inhibition of angiogenesis. PLoS One. 2014;**9**(1):e84249

[17] Baratchart E, Benzekry S, Bikfalvi A, Colin T, Cooley LS, Pineau R, Ribot EJ, Saut O, Souleyreau W. Computational modelling of metastasis development in renal cell carcinoma. PLoS Computational Biology. 2015;**11**(11):e1004626

[18] Stéphanou A, Mcdougall SR, Anderson ARA, Chaplain MAJ. Mathematical modelling of flow in 2D and 3D vascular networks: Applications to anti-angiogenic and chemotherapeutic drug strategies. Mathematical and Computer Modelling. 2005;**41**(10):1137-1156

[19] Wu J, Long Q, Xu S, Padhani AR. Study of tumor blood perfusion and its variation due to vascular normalization by anti-angiogenic therapy based on 3D angiogenic microvasculature. Journal of Biomechanics. 2009;**42**(6):712-721

[20] Soltani M, Chen P. Numerical modeling of interstitial fluid flow coupled with blood flow through a remodeled solid tumor microvascular network. PLoS One. 2013;**8**(6):e67025

[21] Zhao G, Yan W, Chen E, Yu X, Cai W. Numerical simulation of the inhibitory effect of angiostatin on metastatic tumor angiogenesis and microenvironment. Bulletin of Mathematical Biology. 2013;**75**(2):274-287

[22] Wu J, Ding Z, Cai Y, Xu S, Zhao G, Quan L. Simulation of tumor microvasculature and microenvironment response to anti-angiogenic treatment by angiostatin and endostatin. Applied Mathematics and Mechanics. 2011;**32**(4):437-448

[23] Cai Y, Wu J, Gulnar K, Zhang H, Cao J, Xu S, Long Q, Collins MW. Numerical simulation of solid tumor angiogenesis with endostatin treatment: A combined analysis of inhibiting effect of anti-angiogenic factor and micro mechanical environment of extracellular matrix. Applied Mathematics and Mechanics. 2009;**30**(10):1247-1254

[24] Baxter LT, Jain RK. Transport of fluid and macromolecules in tumors. (II) Role of heterogeneous perfusion and lymphatics. Microvascular Research. 1990;**40**:246-263

[25] Zhao G, Wu J, Xu S, Collins MW, Long Q, König CS, Jiang Y, Wang J, Padhani AR. Numerical simulation of blood flow and interstitial fluid pressure in solid tumor microcirculation based on tumor-induced angiogenesis. Acta Mechanica Sinica. 2007;**23**(5):477-483

IntechOpen